Beam Characterization at BATMAN for Variation of the Cs Evaporation Asymmetry and Comparing Two Driver Geometries

E. Aza*, L. Schiesko, C. Wimmer, D. Wünderlich, U. Fantz and the NNBI Team

Max-Planck-Institut für Plasmaphysik (IPP), Boltzmannstr. 2, 85748 Garching, Germany
Corresponding author: eleni.aza@ipp.mpg.de

Abstract The properties of the negative hydrogen ion beam produced by the ITER NBI source at the BATMAN test bed were investigated by means of two diagnostics: Beam Emission Spectroscopy (BES) and a calorimeter. Two modifications to the prototype were applied. The first modification was the installation of a second Cs oven at the bottom part of the source back plate in addition to the standard one at the upper part of the source back plate varying the Cs evaporation asymmetry inside the source. The second modification consisted in the replacement of the cylindrical driver with a larger racetrack-shaped RF driver and installing a single Cs oven in a central position at the back plate of the driver. The resulting beam characteristics are discussed and compared with those obtained with the previous source design. The position of the Cs oven and the different driver size and geometry appear not to influence the beam profile and the beam deflection for a well-conditioned source.

INTRODUCTION

For heating and current drive, one of the key components of ITER NBI system is the negative ion source, generating hydrogen and deuterium negative ions [1]. BATMAN (BAvarian Test MAchine for Negative ions) [2] is a test facility where the prototype ITER NBI source is installed with a size of 1/8 of the ITER source. The negative hydrogen ion beam produced at BATMAN is characterized by diagnostics located at different distances from the extraction system. The five beam emission spectroscopy horizontal lines-of-sight [3] are used to characterize the beam. It is possible to derive from these measurements the local divergence and beam intensity. A second diagnostic is a copper calorimeter [2] measuring with embedded thermocouple and from which one can derive the horizontal and vertical beam profiles as well as beam position. Factors affecting the beam profile are primarily the distribution of the extracted negative ion currents and the negative ion trajectory inclination due to the magnetic fields present in the accelerator and the tank. The effect of these factors is investigated for two modifications applied to the prototype: varying the Cs evaporation asymmetry inside the source and changing the driver geometry. A parallel study focused on the plasma parameters for these modifications was conducted and reported in [4].

BEAM DIAGNOSTICS

Overview of the ion source

The prototype negative hydrogen ion source installed at BATMAN is shown in Figure 1: the plasma ignition and heating takes place in the RF driver, a 14 cm long alumina cylinder with a water-cooled RF coil connected to a 1 MHz oscillator. The plasma expands into the source body, yielding plasma pulses of approximately 7 s with 4.5 s negative ion extraction phases. The area of the source body section (0.32 x 0.59 m^2) is roughly 1/8 of the ITER source area.

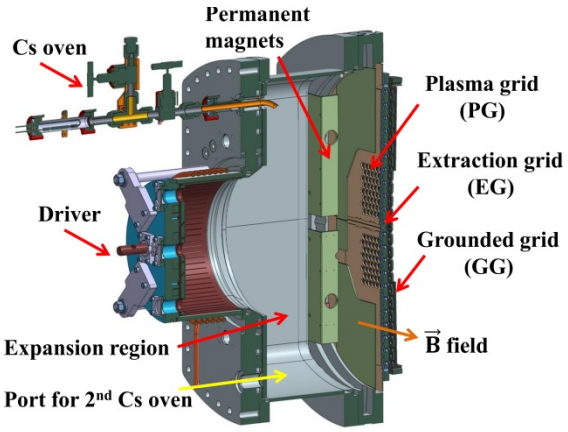

FIGURE 1. The prototype source at BATMAN. The Cs oven is located at the upper part of the backplate and has a cylindrical shape.

Most of the extracted H^- are produced on the plasma grid by conversion of hydrogen atoms and positive ions on the surface of the PG, the first grid of a three-grid, multi-aperture extraction system [5]. The probability of this surface production mechanism depends on the work function of the surface, which can be lowered by covering it with Cs. Caesium is evaporated in the source by an oven located at the upper part of the source back plate, as shown in Figure 1, and redistributed in the source during the plasma pulses.

The extracted negative ions are accelerated by a system of three multi-aperture grids at different potentials: the plasma grid (PG), extraction grid (EG) and the grounded grid (GG) (Figure 1). The geometry of the grids is known as LAG (Large Area Grid), made of two identical halves tilted by 0.9^o each and with 63 apertures each; the apertures are arranged in six rows with alternating 11 or 10 apertures of 0.8 cm diameter and a total extraction area of 63 cm^2. The typical voltage between PG and EG (extraction voltage) varies from 5 to 10 kV and between EG and GG (acceleration voltage) varies from 10 to 15 kV. The extraction of negative ions inevitably leads to the co-extraction of electrons, the amount of which is reduced by permanent magnets installed in front of the PG in order to avoid a too high power load on the EG. In the standard configuration, the resulting magnetic filter field direction [2] leads to a Lorentz force pointing upwards and it is also present in the drift region located downstream the GG.

Once extracted and accelerated the beam enters the drift region, where it is detected by means of two beam diagnostics: a vertical array of five lines-of-sight for spectroscopy (BES) and a copper calorimeter. The beam profile is highly affected by the filter field which deflects the beam upwards with respect to the center of the PG. Another factor possibly affecting the beam profile is the vertical plasma distribution right before the PG, which is shifted upwards by a combination of cross-B drifts. An additional role is played by the Cs asymmetry inside the source, which may result in a non-homogeneous production of negative ions on the PG. At a source pressure of 0.6 Pa, optimum beam optics and well-caesiated source the divergence of the beam is about 4^o.

BEAM EMISSION SPECTROSCOPY (BES)

Beam emission spectroscopy is used to estimate the local intensity and divergence of the beam. This is performed by measuring the Hα Balmer line from the light spectrum emitted after the interaction between the beam and the background gas in the drift region. The spectrum [3] shows two peaks: the Doppler-shifted peak with a wavelength corresponding to light emitted from fully accelerated negative ions interacting with the background gas in the tank and the unshifted Hα line. The light emitted is collected along five horizontal lines-of-sight (LOS), located approximately 0.7 m downstream from the grounded grid and having an angle of $\theta=52^o$ with respect to the beam axis (Figure 2). The vertical distance between the centers of two LOS is 4 cm and the vertical position of the middle LOS corresponds to the center of the PG (0 cm); the five LOS are position-labeled from -8 cm to +8 cm with respect to the PG. Due to the beam divergence, the tilted GG and the distance of the LOS from the GG, the beamlets formed in the extraction system are merging in distance. Thus the LOS see the overlap of many beamlets emerging from the GG and measure only averaged properties along a line-of-sight. The light collected from each LOS is focused to an optic fiber by means of a lens and directed to a spectrometer. Due to the fiber diameter and focal length of the lenses the line-of-sight has a broadening of approximately 0.6^o. The optical system is absolutely

calibrated and the intensity from each LOS is measured from the area of the spectrum under the Doppler peak fitted with a Gaussian distribution.

One of the most important characteristics of the beam is the divergence. The main parameters affecting the beam divergence are the extracted current density and the voltage applied on the extraction and acceleration grids, V_{ex} and V_{acc} respectively. The beam divergence is calculated from the formula: $div=eHWHM/((\lambda_0-x_c)*\tan\theta)$, where eHWHM is the e-folding half width at half maximum of the Gaussian, λ_0 and x_c correspond to the peak wavelength of the unshifted and shifted peaks respectively and θ is the observation angle of the LOS with respect to the axis. The beam divergence is strongly related to the perveance P, defined as the ratio of the extracted ion current I_{ex} to $V_{ex}^{3/2}$. The maximum perveance P_0 corresponds to the maximum possible extracted current I_{ex} limited by the space-charge of the beamlet (Child-Langmuir law) and the normalized perveance is the ratio P/P_0. The dependence of the beam divergence on the normalized perveance is found to be parabolic [3]: for increasing P/P_0 the beam divergence decreases (underperveant region) reaching a minimum and increases in the overperveant region. At BATMAN the source is operated mostly in the underperveant region. As show in figure 2, because there is no overlapping of the BES LOS, the beam intensity and divergence can be resolved locally in the vertical direction.

Copper Calorimeter

The copper calorimeter is located approximately 1.7 m downstream from the grounded grid. It consists of a water-cooled panel 60x60 cm^2 with thermally isolated areas where thermocouples are embedded. The calorimeter permits to obtain the horizontal and vertical beam profile with 29 thermocouples in total arranged as a cross and a distance of 4 cm between them in the vertical and horizontal direction. The temperature difference ΔT is measured for each thermocouple between the start and the end of the beam phase, which is proportional to the power difference ΔP, acquiring the beam profile in 16 positions from -28 cm to 28 cm for each direction (Figure 2). The calorimeter area is large enough to detect almost the entire beam, depending on the angular spread of the particle trajectories around the beamlet axis.

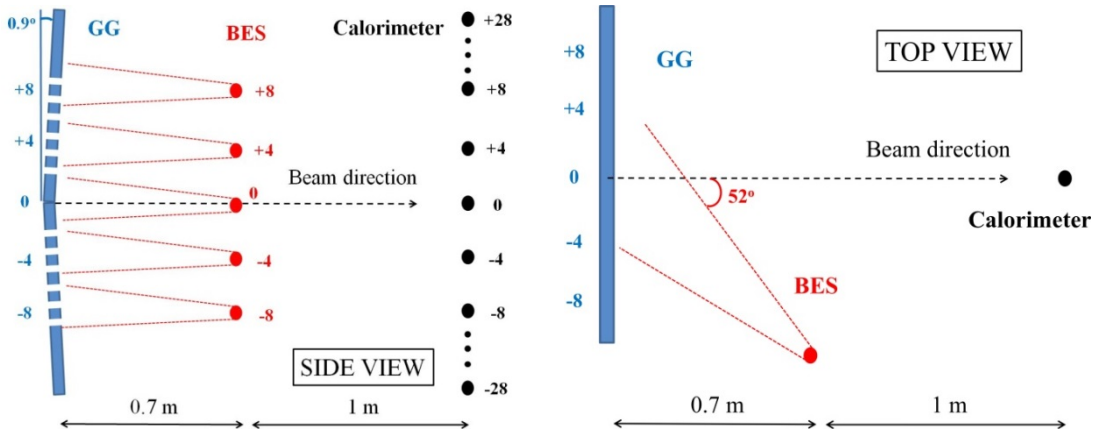

FIGURE 2. Diagnostics set up viewed from the side (left) and the top (right): BES are located at 0.7 m and the calorimeter at 1.7 m from the grounded grid, tilted by 0.9^o. Positions are expressed in cm.

Examples for vertical beam profiles measured with the BES and the calorimeter are shown in Figure 3 for a source pressure of 0.6 Pa, voltages equal to V_{ex}=5 kV and V_{acc}=15 kV and an extracted current density of j_{ex}=21 mA/cm^2. The profile from the calorimeter is fitted with a Gaussian distribution with a peak position at 6 cm, indicating that the beam is deflected upwards with respect to the center of the PG (0 cm). The BES intensities are shown in the five positions from -8 cm to 8 cm.. It can be seen that the profiles acquired with the BES and the calorimeter are not identical in shape; the reason lies in the different distance at which the two diagnostics are located. Since the beam is divergent and the grids tilted, the beamlets merge in distance and the asymmetries are expected to be reduced with increasing distance from the grounded grid [3].

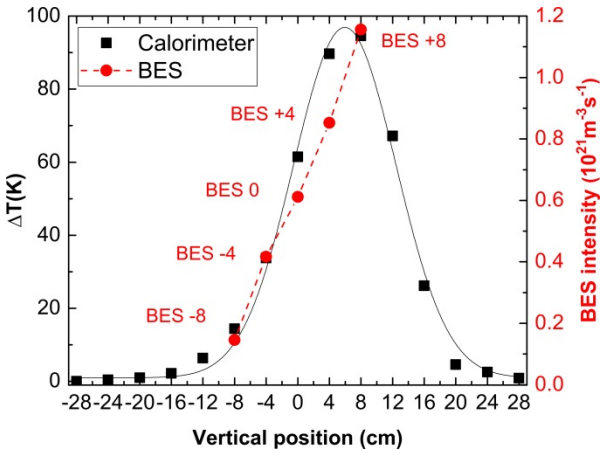

FIGURE 3. Comparison of vertical profiles measured with the BES and the calorimeter for a source pressure of 0.6 Pa, V_{ex}=5 kV and V_{acc}=15 kV and j_{ex}=21 mA/cm^2.

CS EVAPORATION ASYMMETRY

The prototype source consists of a Cs oven installed at the upper part of the source back plate of the expansion region. In this work a second oven was installed at the bottom part of the source back plate. By evaporating from either the top or the bottom oven the Cs asymmetry in front of the PG changes [4]. The possible influence of this asymmetry on the beam profile was investigated with the two beam diagnostics.

During source conditioning the work function on the PG gradually lowers as a result of the Cs coverage, leading to a higher amount of extracted current density j_{ex}. The total light intensity measured from the sum of the five BES LOS and power on the calorimeter via the temperature difference ΔT are increasing linearly for increasing extracted current density during conditioning, as shown in Figure 4. The source pressure was 0.6 Pa and extraction and acceleration voltages were equal to 9 kV and 13 kV respectively, while Cs was evaporated from the top oven.

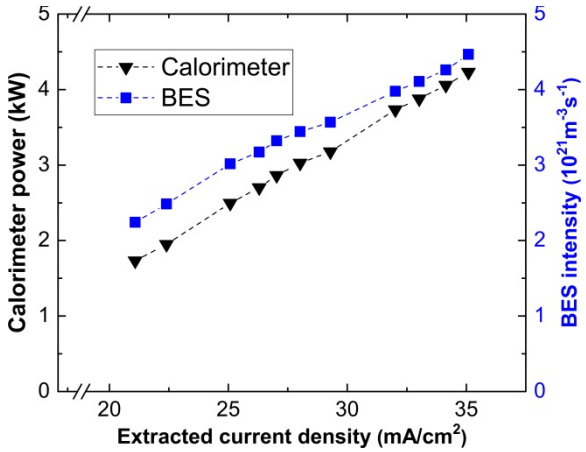

FIGURE 4. Total BES intensity and power on the calorimeter during conditioning and for Cs evaporation from the top oven.

The beam profile evaluated from the BES measurements while conditioning the source with either the top or the bottom oven. The intensity per BES LOS is shown with top and bottom ovens in Figures 5a and 5b respectively for two different random operational days and the same source parameters for increasing extracted current density. The uncertainty in the measurement is 10% and is plotted for a single point.

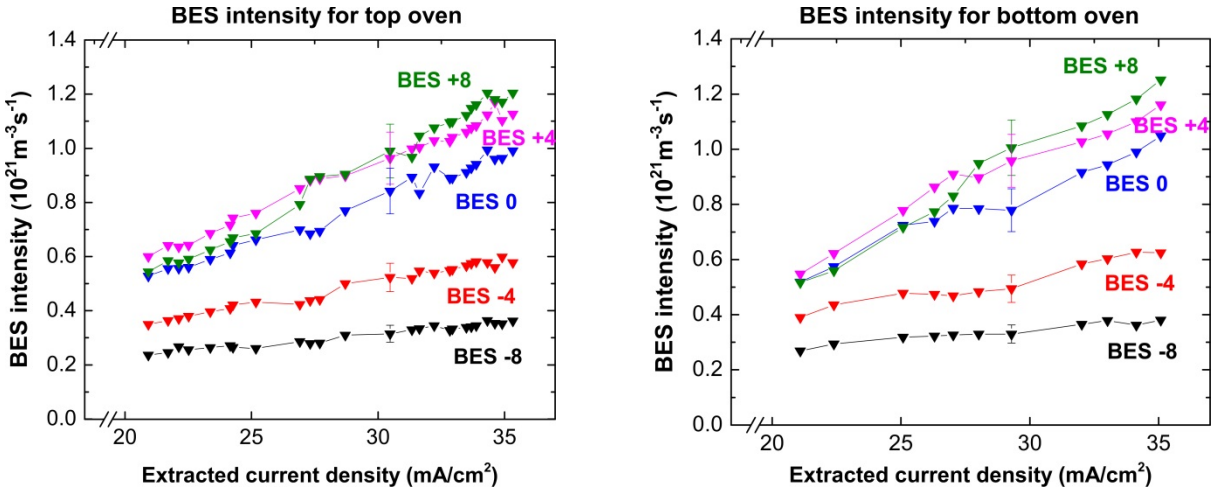

(a) (b)

FIGURE 5. BES intensity per LOS for increasing extracted current density and evaporation only from the top (a) and the bottom oven (b).

It can be seen in both figures that the intensity measured for each BES LOS is increasing during Cs evaporation. However the absolute values vary between the LOS since different parts of the beam are probed and the beam not being homogeneous as shown in Figure 3. For j_{ex} higher than 27 mA/cm^2 BES LOS +8 shows the highest intensity and BES LOS -8 the lowest: this suggests that more current is extracted from the upper part of the PG.. At extracted current density higher than j_{ex}=27 mA/cm^2 the intensity profile measured is the same for evaporation from both the top and the bottom ovens. Tests were performed with evaporation from both ovens at the same time and the beam profile was found to be the same as evaporating from a single oven at high extracted current density and well caesiated source at a source pressure of 0.6 Pa.

The divergence profile of the beam derived from the BES LOS for evaporation from either the top or bottom oven for the data sets in Figures 5a and 5b is shown in Figures 6a and 6b. The divergence for all LOS is decreasing for increasing extracted current density since the source is operated in the underperveant region. For extracted current density higher than 29 mA/cm^2 the divergence per BES LOS is the same for evaporation from either the top or bottom oven.

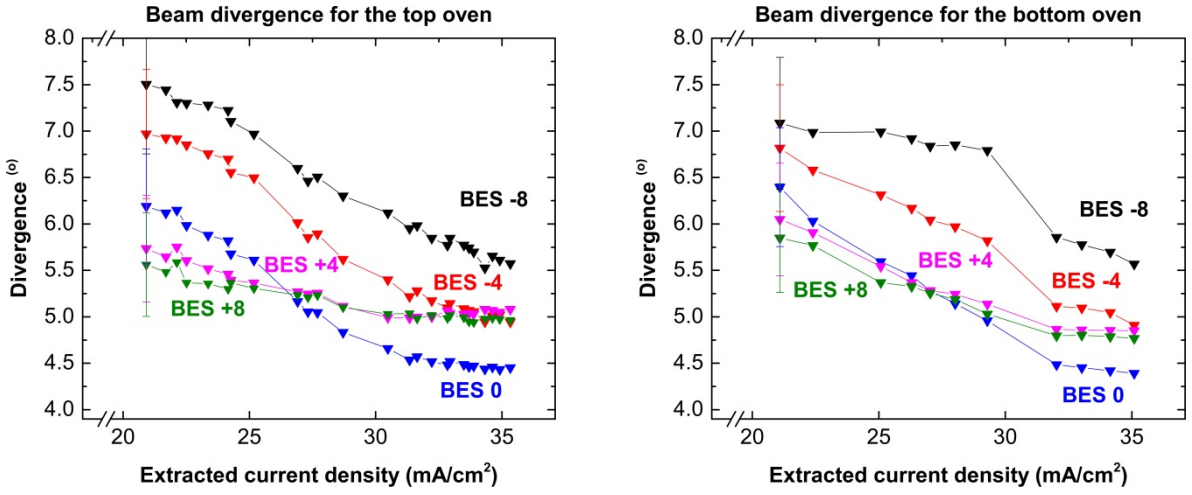

(a) (b)

FIGURE 6. BES divergence per LOS for increasing extracted current density and evaporation only from the top (a) and the bottom oven (b).

The vertical beam position with respect to the center of the PG was measured from the peak position of the profile the calorimeter fitted with a Gaussian distribution. The results are shown in Figure 7a. It can be seen that for increasing extracted current density the beam is shifted upwards by a few centimeters; even though during conditioning the peak position differs for evaporation from either the top or the bottom oven, for j_{ex} higher than 29 mA/cm^2 the beam position is identical for the two ovens. From the light intensity measured for each BES LOS one can estimate the level of beam deviation from the center of the PG. The formula $\nu = ((I_4 + I_5) - (I_1 + I_2))/\sum_{n=1}^{n=5} I_n$, where I_n corresponds to the individual BES LOS intensities, expresses this deviation as total intensity difference measured between top and bottom part of the PG (see Figure 3). A perfectly symmetric beam has a deviation factor ν of zero; for positive ν the beam is shifted to the top. The vertical beam deviation for evaporation from the top and bottom ovens measured by BES is shown in Figure 7b for increasing extracted current density: in agreement with the calorimetric results the factor for both top and bottom ovens is increasing and converging.

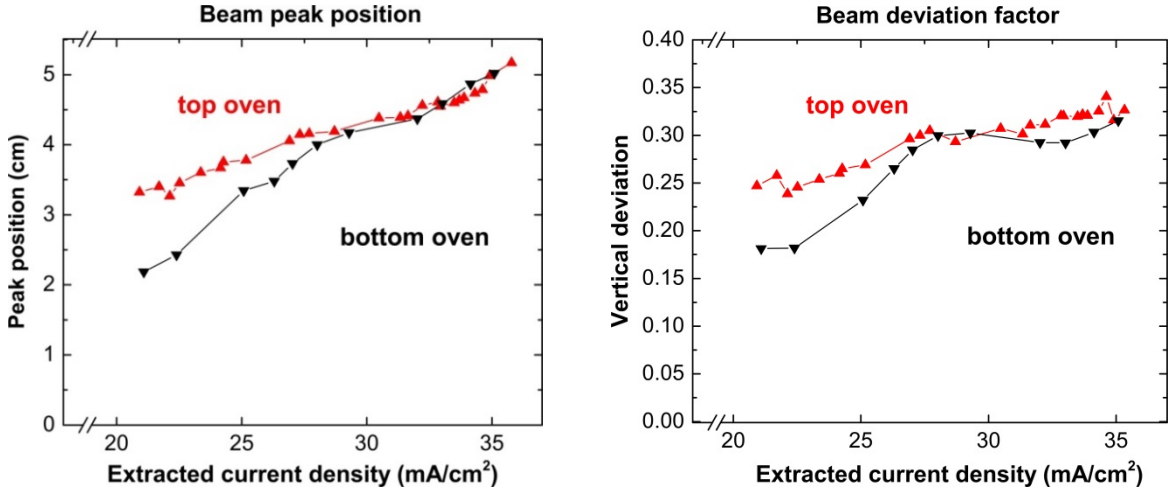

(a) (b)

FIGURE 7. (a) Vertical peak position of the beam measured by the calorimeter with the top and the bottom ovens. (b) Beam deviation factor in the vertical direction measured by the BES with the top and bottom oven.

This study has shown that the vertical beam profile in terms of intensity and divergence is identical after conditioning with either the top or the bottom oven for the same high extracted current density independent from the position of the Cs oven and thus the Cs evaporation asymmetry. This asymmetry does not affect significantly neither the source performance nor the beam asymmetry at 0.6 Pa. Redistribution of Cs by the plasma is adequate enough to achieve sufficient Cs coverage on the full area of the PG and a second oven at the bottom part of the backplate is not needed [4].

COMPARISON OF TWO DRIVER GEOMETRIES

The second modification of the source consists in replacing the cylindrical driver with a larger racetrack-shaped RF driver [6] with a volume 5 times larger than the cylindrical one and installing the Cs oven in a central position at the back of the driver. The main idea is that one racetrack driver could substitute two cylindrical drivers in larger sources with increased reliability and power efficiency [4]. The previous study has shown that the beam profile is not affected by the position of the oven for high extracted current density. However the different shape and larger size of the racetrack driver could result in more homogeneous illumination of the PG, higher ion extraction from the bottom part of the PG.

A comparison between the two different driver geometries was performed using the total intensity measured with the BES for increasing extracted current density during Cs conditioning. The source pressure was 0.6 Pa and extraction and acceleration voltages were equal to 9 kV and 13 kV respectively. The results are shown in Figure 8a. The BES intensity measured is the same for the two drivers. Similar beam profiles were measured with the calorimeter and at 30 mA/cm^2 the comparison can be seen in Figure 8b.

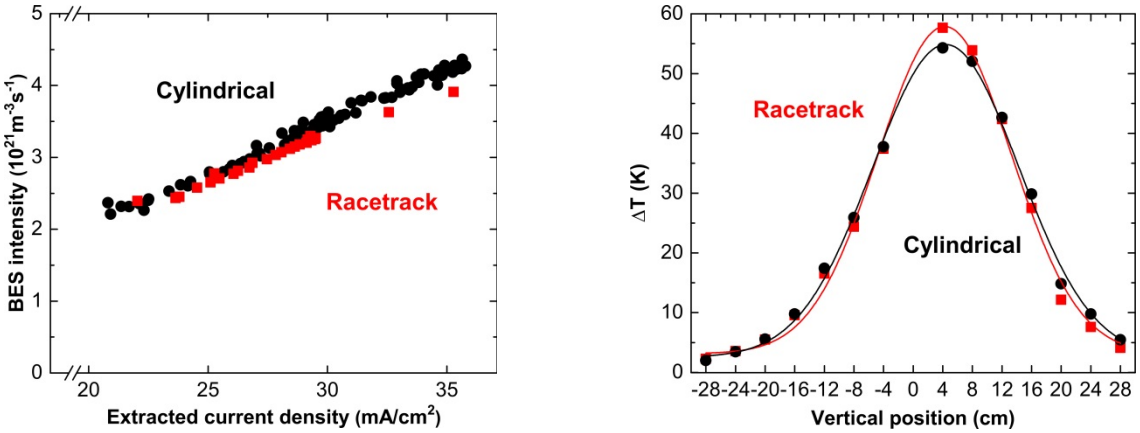

(a) (b)

FIGURE 8. (a) Total BES intensity measured with the cylindrical and racetrack drivers for increasing extracted current density. (b) Comparison of beam profiles measured with the calorimeter for the two drivers at j_{ex}=30 mA/cm^2.

The same trend was found with the BES at 30 mA/cm^2: the vertical profiles of total BES intensities and divergence are similar for the two driver geometries (Figures 9a and 9b). This means that the beam produced using the racetrack driver has comparable characteristics as the cylindrical one in terms of intensity and divergence and the larger size of the racetrack driver has no effect on the beam profile. Since the Cs evaporation asymmetry does not influence the beam profile and the plasma distribution in front of the PG appears to be the same for the two drivers [4], it can be concluded that the beam profile is solely determined by the magnetic filter field.

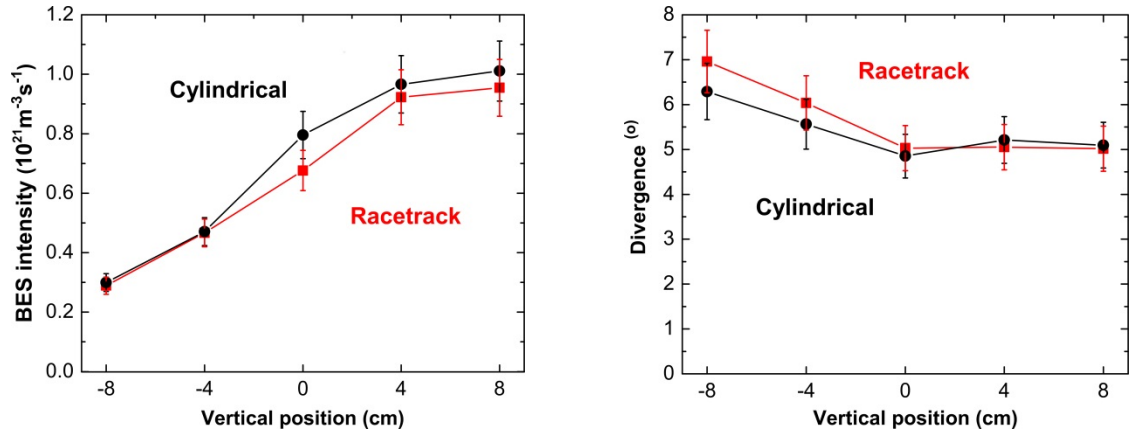

(a) (b)

FIGURE 9. Comparison of beam profiles measured with the BES for the two drivers in terms of intensity (a) and divergence (b).

CONCLUSIONS

The profile of the hydrogen ion beam at BATMAN was investigated with modifications applied to the standard prototype source. The prototype source consists of a cylindrical driver and a Cs located at the upper part of the source back plate. For the needs of this study a second oven was installed at the bottom part of the source back plate. When evaporating Cs exclusively from one of these ovens the Cs asymmetry inside the source changes but the vertical beam profile appears to remain unaffected: the beam intensity, divergence and position are the same for evaporation from either oven in particular after Cs-conditioning. The second modification in the source consists in replacing the cylindrical driver with a larger racetrack-shaped RF driver and placing the Cs oven in a central position at the back of the driver. Despite the larger size and different shape of the racetrack driver, the beam profile

was found to be the same as with the cylindrical driver. Therefore the beam profile appears to be determined only from the magnetic filter field.

ACKNOWLEDGMENTS

This work has been carried out within the framework of the EUROfusion Consortium and has received funding from the Euratom research and training programme 2014-2018 under grant agreement No 633053. The views and opinions expressed herein do not necessarily reflect those of the European Commission.

REFERENCES

[1] R. Hemsworth, A, Tanga and V. Antoni, Rev. Sci. Instrum. **79**, 02C109 (2008).
[2] E. Speth, H.D. Falter, P. Franzen, U. Fantz, M. Bandyopadhyay, S. Christ, A. Encheva, M. Froschle, D. Holtum, B. Heinemann, W. Kraus, A. Lorenz, Ch. Martens, P. McNeely, S. Obermayer, R. Riedl, R. Suss, A. Tanga, R. Wilhelm and D. Wunderlich, Nucl. Fusion **46**, p. S220 (2006).
[3] R. Maurizio, U. Fantz, F. Bonomo and G. Serianni, Nucl. Fusion **56**, 066012 (2016).
[4] C. Wimmer, U. Fantz, E. Aza, J. Jovovic, W. Kraus, A. Mimo and L. Schiesko, Contribution to the NIBS 2016 conference, **this volume** (2016).
[5] M. Bacal and M. Wada, Appl. Phys. Rev. **2**, p. 0213052015
[6] W. Kraus, U. Fantz, B. Heinemann, L. Schiesko and C. Wimmer, **this volume** (2016).